BULLETIN OF THE POLISH ACADEMY OF SCIENCES
TECHNICAL SCIENCES, Vol. 68, No. 3, 2020
DOI: 10.24425/bpasts.2020.133379



# Manufacturing of $ZrO_2$-Ni graded composites via centrifugal casting in the magnetic field

M. WACHOWSKI[1], R. KOSTUREK[1], H. WINKLER[2], A. MIAZGA[2], P. LADA[2], W. KASZUWARA[2], K. KONOPKA[2], and J. ZYGMUNTOWICZ[2]*

[1] Military University of Technology, Faculty of Mechanical Engineering, 2 Gen. S. Kaliskiego St., 00-908 Warsaw, Poland

[2] Warsaw University of Technology, Faculty of Materials Science and Engineering, Woloska 141 St., 02-507 Warsaw, Poland

**Abstract.** The paper presents the possibility of fabricating ceramic-metal composites by an innovative method of centrifugal slip casting in the magnetic field. It was examined whether the use of this method would allow obtaining a gradient concentration of metal particles in the ceramic matrix. In the applied technique, the horizontal rotation axis was used. The study investigated the effect of solid phase content on the properties and microstructure of the products. Water-based suspensions with 35, 40, 45 and 50 vol.% of solid-phase content were prepared with 10 vol.% additional of nickel powder. The viscosity of prepared slurries was considered. The gradient distribution of nickel particles in the zirconia matrix was observed on SEM. Vickers hardness of $ZrO_2$-Ni composites has been measured. The research revealed that the physical properties depend on the volume fraction of solid content and increase as the volume of solid content increases.

**Key words:** $ZrO_2$-Ni, ceramic matrix composites, FGM, microstructure, magnetic field.

## 1. Introduction

Due to their unique properties, functionally graded materials (FGM) have been gaining great interest in recent years [1–4]. In these materials, along the at least one specific direction, a continuous change in constructional and/or performance properties has been achieved using a selected technological process [5–6]. The type of obtained gradient depends on many parameters and the priority factors determining the structure of the gradient are, among others: the type of technology used; density of components; solid phase content in the slurry; type, size and chemical composition of the used components [7]. The idea of graded materials was first described by Devez and Bever in 1971, but intensive development in this field was initiated in the 90s [6–9]. Depending on the type of the starting components, functional gradient materials can be divided into three material groups: ceramic-metal, polymer-ceramic, metal-metal. Literature data indicate that the distribution gradient of the phase dispersed into the matrix can have a wide volume range [10]. Depending on the distribution of the phase in the matrix, FGM can be distinguished by the fact that the particle gradient is located only at the external surface of materials in which the gradient is observed along the entire longitudinal or transversal section [11]. Another type of division of this material group is due to the geometry of the gradient system as one-dimensional, two-dimensional and three-dimensional with different types of symmetry: axial, radial or cylindrical [12]. Depending on the type of material used and the assumed initial criteria of the FGM shaping process, gradient materials with different utility properties can be obtained. The main characteristic feature of such materials is the gradient of physical and chemical properties, which determine material behavior under operating conditions. Literature data show that by comparing FGM to a composite without a gradient formed by joining, for example by welding two components (e.g., ceramic and metal), the interface properties change stepwise in the case of the composite obtained by welding [13]. This can cause numerous defects (such as microcracks) and consequently lead to the instability of such products, in particular when they are exposed to operating processes at elevated temperatures [14]. The use of gradient materials leads to a reduction in costs associated with the operation and maintenance of structural components. Functional gradient materials can be applied as materials for turbine blades, biomaterials, thermal barriers, or pipes for the transport of toxic medium [15–18]. Despite such a great potential of these materials as engineering materials, they are still the subject of basic research, particularly in terms of the relation between the parameters of the technological process and the distribution of metal particles in obtained composites. Understanding these relationships will allow for controlling the production of structures with a gradient depending on the needs and the required material properties. In particular, the determination of dependencies between the formation of a gradient (e.g. in the form of a concentration gradient of metal particles in a ceramic matrix) and specific technological parameters is an important factor from the manufacturing point of view. These relations are directly linked to the type of composite production method, in selection of which an economic aspect plays a key role. What is more, a significant emphasis is put on high repeatability as well as the performance of the used production technique. In the case of FGM, the change of properties takes place continuously, which allows for using such materials, among others, for the production of tools for cold and hot plastic forming [19], gradient tool materials [20], as well as for the production of parts in the aerospace and automotive industries [21]. Another

*e-mail: justyna.zygmuntowicz@pw.edu.pl

Manuscript submitted 2019-09-16, revised 2019-11-21, initially accepted for publication 2020-02-02, published in June 2020

application of functional gradient materials is the production of anti-reflective layers, lenses or other protection elements in optoelectronics [22]. According to the current state of knowledge based on literature data, gradient materials (FGM) can be obtained by many methods, such as impulse laser deposition method, powder injection molding, infiltration process, laser sintering, laminating, spray molding, electrolytic deposition, plasma spraying, centrifugal slip casting, slip casting with the use of the magnetic field, a suspension coating or a self-supporting high-temperature synthesis method [23–30]. The results of research on the use of the centrifugal slip casting method in the magnetic field to produce composites from the ceramic-metal system ($Al_2O_3$-Ni) show the utility of this technology for shaping elements with controlled distribution of metal particles in a ceramic matrix [31]. Although the typical centrifugal casting is a technology traditionally used in the casting of metals and their alloys, due to the high demand for modern materials with advanced properties, attempts are made to obtain gradient composite materials by centrifugal casting, using the effect of centrifugal force. This technique is most often used for fabricating metal-ceramic composites and involves the introduction of ceramic particles into the liquid metal; then the prepared mass is poured into a solid mold and subjected to a solidification process [32]. The method of centrifugal slip casting in the magnetic field combines the classic casting of the slurries with the effect of centrifugal force, as well as the simultaneous action of the magnetic field [13, 31]. As a result of the use of porous plaster molds, the liquid medium is removed from the suspension, which in turn leads to a thickening of the material. At the same time, centrifugal force causes simultaneous variable deployment of metal particles in the ceramic matrix. Applying magnetic field allows for a controlled change in the distribution of the metallic phase in the composite. In the case of FGM production, the most important factor is the difference in the densities of the starting materials used. The proposed method can be an interesting alternative to the existing methods for obtaining gradient composites. Previous research work related to the production and characteristics of ceramic-metal composites by centrifugal slip casting process concerned mainly the $Al_2O_3$-Ni system [13, 31, 33]. This investigation concentrates on $ZrO_2$-Ni system, which is a very promising composite. Its coefficient of thermal expansion and elastic modulus of components allow for limiting the stress occurring on ceramic-metal particle boundary and in consequences to minimalize the risk of failure, particularly during operating at an elevated temperature. An additional advantage of the considered system is its high chemical stability since $ZrO_2$ and Ni do not react with each other. The main aim of this article is to fabricate composites from the $ZrO_2$-Ni system with a metallic phase gradient by centrifugal slip casting using a magnetic field and to examine the effect of solid phase content on microstructure and selected properties of obtained composites. Research examines the possibility of controlling the distribution of the metallic phase in the matrix during the forming process as a result of changing the solid phase content in the initial slurry used to fabricate composites. The obtained results allow to determine the relation between microstructure, phase structure and the basic properties of the produced composites.

## 2. Experimental

**2.1. Materials.** In the current work, the $ZrO_2$-Ni functionally graded materials were fabricated by centrifugal casting in the magnetic field. The following substrates were used: commercial $ZrO_2$ TZ-3YS-E powder (TOSOH) with 99.99% chemical purity and commercial Ni powder (Sigma-Aldrich) with 99.99% chemical purity. The zirconia powder was stabilized by 3 mol% $Y_2O_3$. The densities of used powders were measured on a helium pycnometer, AccuPyc II 1340 (Micromeritics), in a sequence of 100 purges and 100 measurement cycles. The results of density measurement from helium pycnometer reveal that the $ZrO_2$ has a density equal to 5.92 g/cm$^3$, while the Ni is characterized by density equal to 8.90 g/cm$^3$. Both powders were shown in Fig. 1. The SEM image (Fig. 1a) reveals that

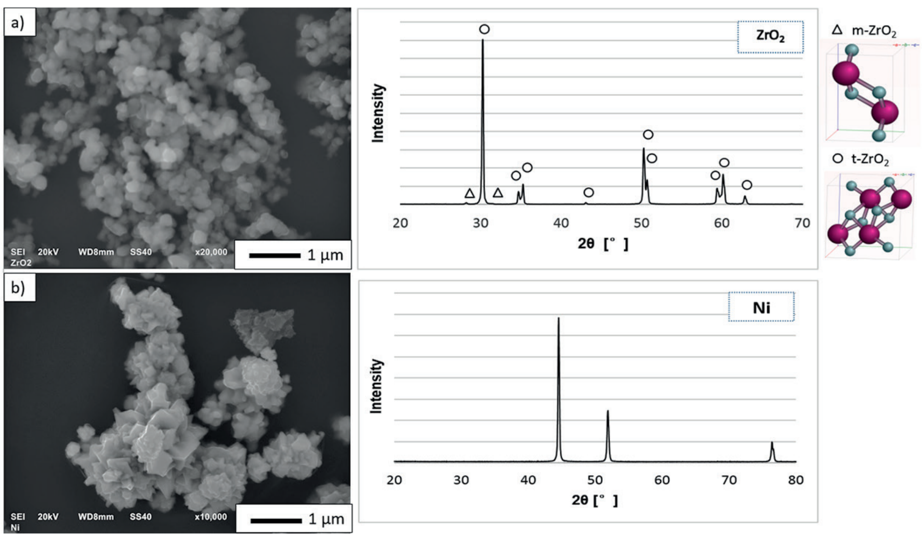


Fig. 1. Morphology and XRD of raw powders: a) $ZrO_2$, b) Ni

the $ZrO_2$ particles are characterized by spherical morphology. It was found that both powders were firmly agglomerated. Moreover, based on SEM images, it has been observed that the Ni powder is characterized by irregular shape (Fig. 1b). XRD analysis reveals that the zirconia oxide contained two phases: tetragonal (t-$ZrO_2$, characteristic card PDF# 04-055-4504) and monoclinic (m-$ZrO_2$, characteristic card PDF# 04-010-6452). Two zirconia phases are the effect of the partial stabilization by 3 mol.% yttrium oxide. In the monolith zirconia ceramic powder, the 64.9 wt.% of tetragonal zirconia and 35.1 wt.% of monoclinic zirconia were identified.

Particle size distribution (PSD) of the raw materials was determined by the laser diffraction technique with the use of Analyzer LA 950 Horiba. A small amount (a few mg) of $ZrO_2$ powder was dispersed in a water medium, while Ni powder was dispersed in an isopropyl alcohol medium. The powders were analyzed by two laser beams: blue (with a wavelength of 460 nm) and red (with a wavelength of 630 nm). The remanence, coercivity and the saturation magnetization measurements for raw powders were taken by vibrating sample magnetometer (VSM) at room temperature. Figure 2 shows the results of magnetization measurements for $ZrO_2$ and Ni powders. The magnetic hysteresis loop of the Ni powder indicates ferromagnetism, while the $ZrO_2$ powder is characterized by diamagnetic properties. The powder samples show coercivity (Hci) of about 99.35 Oe. Furthermore, the nickel was characterized by magnetization (Ms) equal to 0.14137 emu/g and retentivity (Mr) 6.7945 emu/g. The obtained results suggest that the Ni powder should be affected by the magnetic field used in the manufacturing process due to its ferromagnetic character.

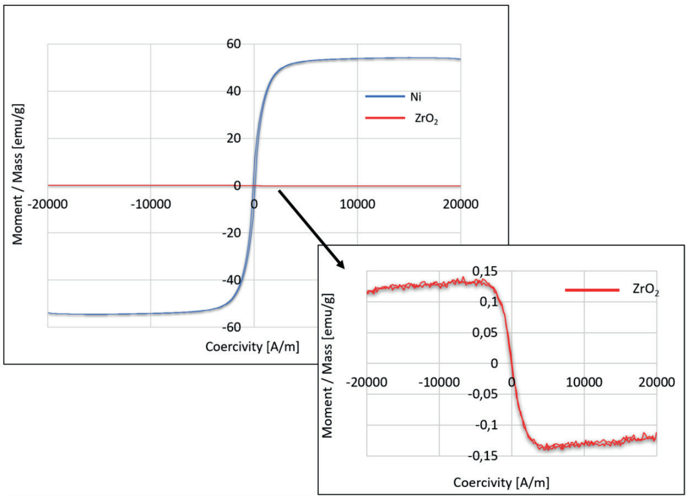


Fig. 2. The hysteresis loops of $ZrO_2$ and Ni

**2.2. Methodology.** In the experimental part, the aqueous ceramic slurries containing 35 vol.%, 40 vol.%, 45 vol.% and 50 vol.% of the solid phase and 10 vol.% of the Ni particles (with respect to the total amount of the solid volume) were examined. Different content of the solid phase in slurries results in different distances between particles in suspensions and differences in the mobility of particles under the influence of centrifugal force and magnetic field. By controlling the content of the solid phase in the suspensions it will be possible to control the final microstructure of the obtaining composites. The composite samples have been obtained in a few steps, starting with the preparation of the composite slurry. Deionized Milli-Q water was used as a solvent, while Diammonium hydrocitrate, DAC (puriss, POCh, Poland) and Citrate acid, CA (puriss, POCh, Poland) were used as dispersing agents. Dispersant (CA and DAC) were dissolved in deionized water. In the next step, the appropriate amounts of metal and ceramic powders have been added into the suspensions. The composition of the used composite slurry is presented in Table 1. According to the invention, the method of producing ceramic-metal composites with a gradient of the Ni particle concentration consists of preparing the slurry and then homogenization in a high-revolution homogenizer. Then the homogeneous mixture is poured into a die and processed in a specially designed apparatus using centrifugal casting in the magnetic field. The picture of the equipment used to fabricate the samples is shown in Fig. 3. Outside the Teflon mold, the Nd-Fe-B magnets fabricate by Euromagnesy (Poland) company were placed in order to generate a magnetic field during the process. These magnets create a very strong magnetic field outside of the mold equal to 550 mT. The distribution of the

Table 1
Compositions of $ZrO_2$-Ni suspensions used in the investigation

| **Total solid content** | **Ni** | **DAC** | **CA** |
|---|---|---|---|
| vol.% | vol.% with respect to the total amount of the solid volume | wt.% with respect to the amount of the ceramic powder ($ZrO_2$) | |
| 35 | 10 | 0.3 | 0.1 |
| 40 | 10 | 0.3 | 0.1 |
| 45 | 10 | 0.3 | 0.1 |
| 50 | 10 | 0.3 | 0.1 |

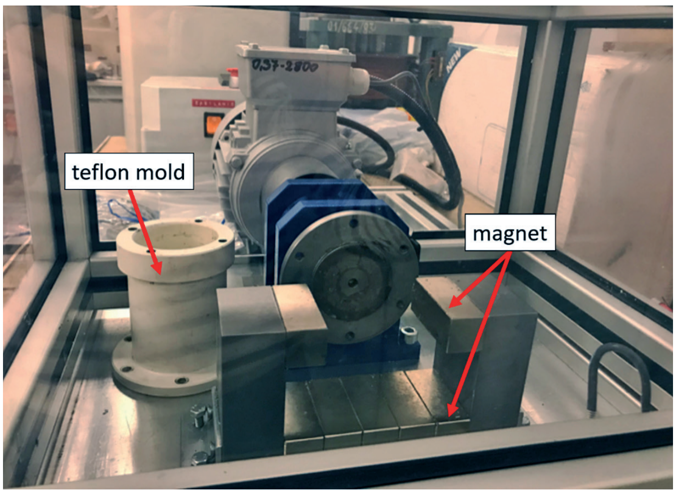


Fig. 3. The equipment used to produce the samples $ZrO_2$-Ni

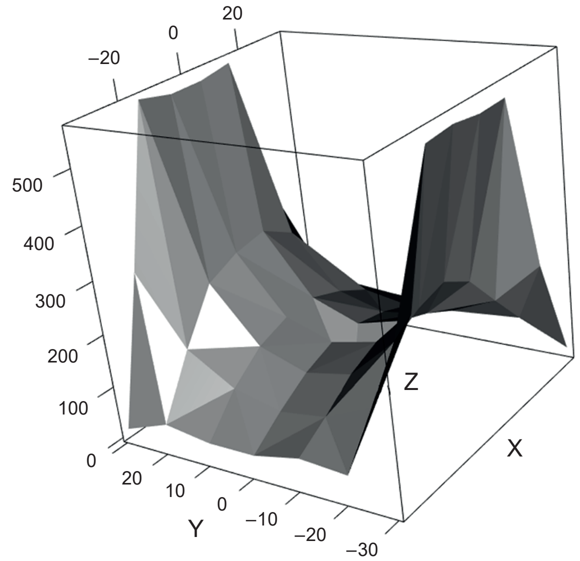


Fig. 4. The distribution of the magnetic field around the mold

magnetic field around the mold is shown in Fig. 4. The magnetic field generates a high attraction force for nickel particles. The strength of the magnetic field to manufacture the composites during the trials was measured by Teslametr HGS-10 A. The rotational speed of the die is selected depending on the composition of the slurry. Then the sample is removed from the die and placed in an oven to burn out the organic additives and sinter the material. The specimens were sintered at 1400°C for 2h in the $H_2/N_2$ atmosphere, a heating rate was 5°C/min. according to the experimental, that method allows for producing a solid composite green body in the form of a sleeve which represents precisely the shape of the die.

Several methods were used to determine properties of the suspensions and microstructure and properties of the final $ZrO_2$-Ni tubes. The rheological measurements are a greatly serviceable method for studying viscosity as a function of the applied shear rate. Based on the rheological measurements, it can be inferred which fabricated slurry has the highest or lowest viscosity. For this purpose, the viscosity of suspensions was measured by the Kinexus Pro rheometer (Malvern Instruments UK) equipped with plate-plate geometry. The diameter of the rotating geometry was 40 mm with the gap between plates equal to 0.5 mm. During the experiment, the value of shear rate was increased from 0.1 to 500 $s^{-1}$. The measurements were done at 25°C. X-ray diffraction analysis was performed using a Rigaku MiniFlex II diffractometer with a Cu-K$\alpha$ radiation source (wavelength $\lambda = 0.154178$ nm) with: voltage 30 kV, current 15 mA, angular range 2θ: 20°–80°, step 0.02° and counting time 0.5 s. The analyses were done at the cross-sections of $ZrO_2$-Ni composites. The physical properties of the obtained $ZrO_2$-Ni materials such as density open porosity were measured by the Archimedes method. In order to investigate the microstructure of the composites, samples were examined using scanning electron microscope (Jeol JSM-6610). SEM observations were carried out using 20 kV acceleration voltage. As the part of metallographic sample preparation, samples were cut along the axial direction using precision diamond saw and then mounted in resin, grinded with abrasive paper of 80, 320, 600, 1200 and 2400 gradations and polished using diamond pastes (3 μm and 1 μm gradation).

## 3. Results and discussion

It is well known that the behavior of the fluid is divided into non-Newtonian and Newtonian flow due to the rheological characteristics. The rheological characteristics of non-Newtonian fluids depend on time or shear rate, while the Newtonian fluids are characterized by stable rheology properties independents on time. In order to characterize the type of slurries used to produce composites, the viscosity of suspensions in shear rate function was measured. Also, another aim of the measurement was to analyze the influence of the solid content on the rheological properties of the slurries. Fig. 5 presents the viscosity curves of the obtained composite slurries. It should be noted that all analyzed slurries were shear-thinning fluids. The value of the initial viscosity of the suspension containing 50 vol.% of solid phase is higher than of all suspensions, which corresponds to the higher concentration of powders in the slurry.

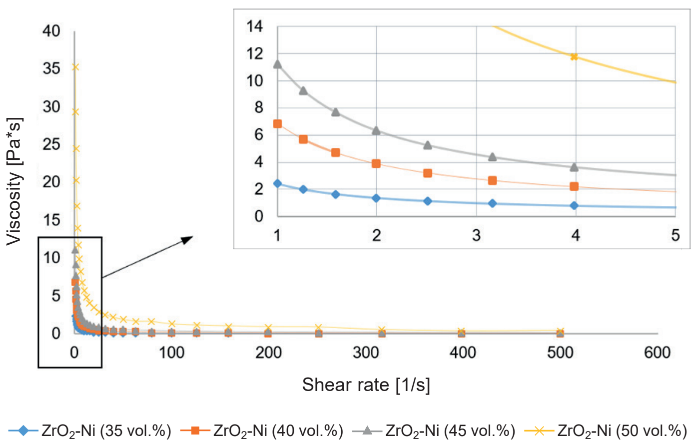


Fig. 5. The viscosity of the prepared suspensions with different concentration of solid phase and 10 vol.% Ni content as a function of shear rate

Figure 6 presents an exemplary diffraction pattern of the sintered composites with 50 vol.% content of the solid phase. XRD analysis revealed no other reflections than those of Ni, t-$ZrO_2$ and m-$ZrO_2$ in all samples (35 vol.%, 40 vol.%, 45 vol.%, 50 vol.% of the solid phase). It was found that the t-$ZrO_2$ (characteristic card PDF# 04-055-4504) phase content was equal to 86.7 wt.%, while the m-$ZrO_2$ (characteristic card PDF# 04–010–6452) accounted for 2.6 wt.%. The additional stabilization of zirconia powder by $Y_2O_3$ ensured a high amount of tetragonal phase (t-$ZrO_2$) after the sintering process, when the temperature of the phase changes (monoclinic m → tetragonal t, over 1170°C) was exceeded. A low amount of monoclinic zirconia in the sintered samples could be the effect of the prepa-

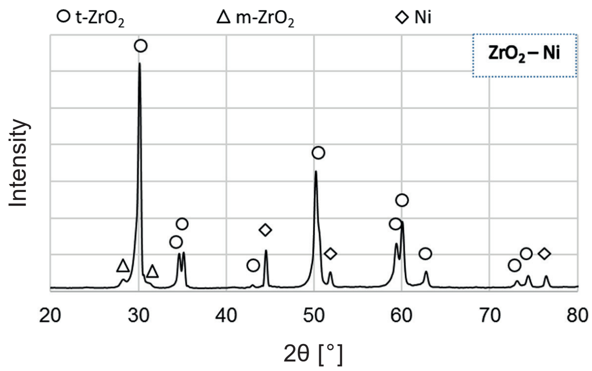


Fig. 6. XRD diffractogram of $ZrO_2$-Ni composites with 50 vol.%

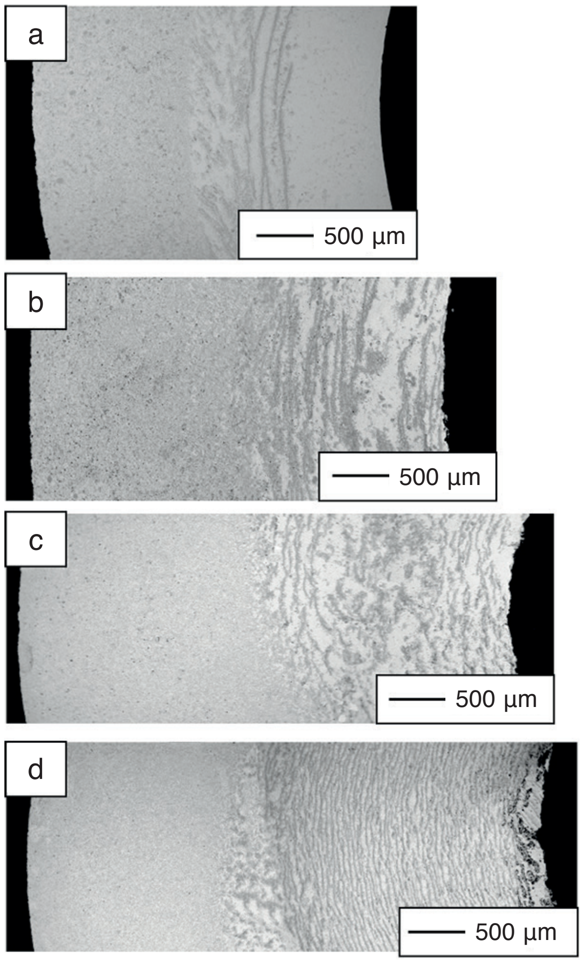


Fig. 7. SEM images of $ZrO_2$-Ni sintered composites obtained from the suspensions containing: a) 35 vol.%, b) 40 vol.%, c) 45 vol.%, d) 50 vol.%.

ration process of the samples for the observations and phase analysis which was conducted on the polish surface and applied loads and water caused the reverse transformation (t → m). The nickel (characteristic card PDF# 70-1849) content was about 10.2–10.7 wt.% in all analyzed composites.

The selected physical properties such as density, open porosity and shrinkage have been measured for the obtained sintered samples. The results of the measurements are shown in Table 2.

The obtained samples have the shape of hollow cylinders, while each composite is characterized by the different diameter of the cylinder and different thickness of the cylinder wall due to the different solid phase content in the initial slurry during the manufacturing process. The microscopic observations were carried out on cross-sectioned fragments of the composites and the images are shown in Fig. 7. It has been reported that the distribution of the metallic phase in the analyzed sample has non-homogeneous character. The darker areas revealed on the micrographs correspond to the nickel phase, while the bright areas are $ZrO_2$ matrix. It was found that the content of the metallic phase changes from the outside to the inner edge of the samples and the character of changes is different for each sample. Observation of the cross-section of the composite obtained with the 35 vol.% of the solid phase concentration revealed the hollow sphere sample with the smallest diameter as compared to other investigated samples. The wall thickness of the cylinder of this sample is approximately 3.0 mm while the diameter of the sample with the hole is 6.7 mm. In 35 vol.% $ZrO_2$-Ni composite, four zones with varying nickel content on the cross-section of the samples were distinguished. It was observed that with decreasing distance from the outer part of the sample, the content of the nickel phase decreases. The highest content of nickel was noted in the area from the outer side up to the middle part of the composite (width 1.3 mm). Metallic particles are located uniformly in this area and the volume content is higher than the content of $ZrO_2$ matrix. In the second zone with the width of 0.5 mm metallic phases are distributed in visible linearity pattern but without specific orientation. The observation of the third zone of the composite revealed the linearity of the nickel distribution with the parallel orientation to the outer edge

Table 2
Properties of obtained $ZrO_2$-Ni composites

| Physical properties | Samples with different content of solid phase in the composites | | | |
|---|---|---|---|---|
| | 35 vol.% | 40 vol.% | 45 vol.% | 50 vol.% |
| Relative density [%] | 88.80 ± 1.23 | 89.48 ± 1.35 | 89.47 ± 1.13 | 90.41 ± 0.93 |
| Open porosity [%] | 10.53 ± 0.34 | 9.11 ± 0.12 | 9.10 ± 0.46 | 9.95 ± 1.02 |
| Linear shrinkage (sample height) [%] | 16.49 ± 0.12 | 18.4 ± 0.13 | 18.19 ± 0.11 | 17.40 ± 0.12 |
| Linear shrinkage (sample diameter) [%] | 43.28 ± 0.39 | 46.56 ± 0.42 | 44.73 ± 0.40 | 41.67 ± 0.38 |

of the sample. The width of the third zone is approximately 0.3 mm. The fourth zone with width 0.9 mm corresponds to pure $ZrO_2$ structure. The hollow sphere sample of the composite obtained with 40 vol.% of the solid phase concentration is characterized by the diameter of 8 mm and thickness of the wall equal to 3.6 mm. Two zones having different concentration of the metallic phases can be distinguished. The area from the outer side of the sample to the center of the sample with width 1.8 mm is characterized by the low concentration of the nickel phase, while the observations of the second zone (also with width of approximately 1.8 mm) revealed the linear distribution of the nickel particles with unsystematic localization. The cross-section of the composite obtained with the 45 vol.% of the solid phase concentration can also be divided into two zones depending on the nickel content. The first zone with the width of 2.1 mm is characterized by the lower nickel content in comparison to the second zone and the metallic particles are located uniformly in this area. Higher content of the nickel was observed in the second zone with the width of 2.1 mm. Metallic phases in the second zone are distributed in visible linearity pattern but without specific orientation. The diameter of this sample with a hole is approximately 9.2 mm and the thickness of the cylinder wall is equal to 4.2 mm. The cross-section of the last composite obtained with 50 vol.% of the solid phase is characterized by the diameter equal to 9.6 mm and the thickness of the cylinder wall is 4.4 mm. In terms of the composite microstructure, three zones with different content of the nickel phase can be characterized. The first zone with a width of approximately 1.7 mm has the lowest content of the nickel phase. The concentration of the nickel increases in the second zone, where the metallic phase is randomly distributed in the area of 0.4 mm width. The third zone with the width of 2.3 mm is characterized by the linear distribution of the nickel phase in the matrix with the lines oriented parallel to the outer edge of the sample.

The obtained results of hardness analysis are presented in Fig. 8. It has been reported that in the case of 35 vol.% sample, the highest fluctuations in hardness occur as a result of microstructure heterogeneity. The high value of hardness (31 GPa) corresponds to the zone consists fully of $ZrO_2$, while the lowest values (21 GPa) are present in the area of high participation of nickel. For samples manufactured with higher input concentration of solid phase (40–50 vol.%), all measured hardness values consist within the range of 18–23 GPa.

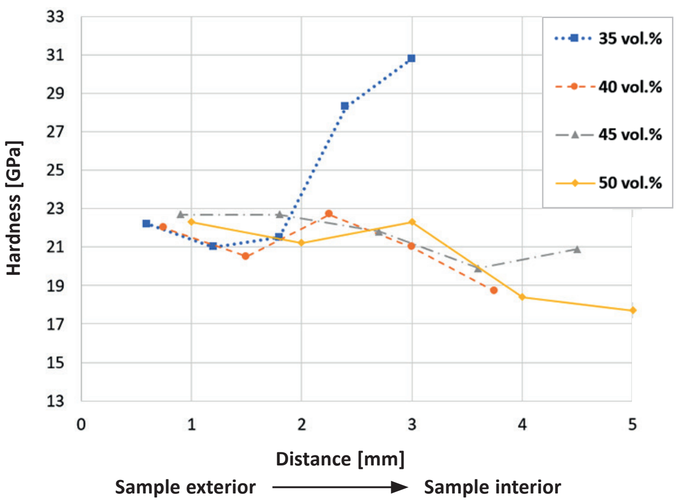


Fig.8. Hardness distribution in the analyzed samples

## 4. Conclusions

$ZrO_2$-Ni graded composites obtained by centrifugal casting in the magnetic field have chemical composition stability during manufacturing process, which has been confirmed by XRD analysis. Additionally, the manufactured composites are free of cracks. The results of this research indicate that for four different concentration values of the solid phase in the slurry, the relative density and open porosity of the composites are on a similar level of 89.5% and 9.6%, respectively. Scanning electron microscopy observations of the composite microstructures allowed for identifying the specific areas characterized by differences in participation of Ni and $ZrO_2$ phases. The highest gradient of concentration has been obtained in the sample with 35% solid phase in the slurry, which also was characterized by the lowest value of viscosity. The gradient finds its reflection in the measured hardness distribution, in which hardness value decreases from 31 GPa to 13 GPa along with increasing Ni phase participation starting from the pure $ZrO_2$ phase. For samples with a higher concentration of solid phase, the microstructure as well as the hardness distribution are more homogeneous, and an area consisting of pure $ZrO_2$ cannot be observed. Despite the slurry solid phase concentration, in all analyzed composites there is a zone where the metallic phase is distributed in the linearity pattern orientated parallelly to the outer edge of the sample.

**Acknowledgements.** The study was accomplished thanks to the funds allotted by The Faculty of Material Science and Engineering, Warsaw University of Technology, within the framework of the research statute work and dean grant no. 6424E-365/M/2018. This investigation supported by the Foundation for Polish Science (FNP).

## References

[1] S. Suresh and A. Mortensen, *Fundamentals of Functionally Graded Materials*, Cambridge University Press, Cambridge, 1998.

[2] Y. Miyamoto, W.A. Kaysser, B.H. Rabin, A. Kawasaki, and R.G. Ford, *Functionally graded materials, design, processing and applications*, Kluwer Academic Publishers, Boston, 1999.

[3] A. Kawasaki and R. Watanabe, "Concept and P/M fabrication of functionally gradient materials", *Ceram. Int.* 23, 73–83 (1997). https://doi.org/73-83.10.1016/0272-8842(95)00143-3.

[4] S. Suresh and A. Mortensen, *Fundamentals of Functionally Graded Materials: Processing and Thermomechanical Behaviour of Graded Metals and Metal-ceramic Composites*, IOM Communications, London, 1998.

[5] K. Hodor, P. Zięba, and B. Olszowska-Sobieraj, "Materiały gradientowe jako nowe możliwości współczesnej techniki", *Inż. Mater.* 6, 595–600 (1999) [in Polish].

[6] M.B. Bever and P.E. Duwez, "Gradients in composite materials", *Mater. Sci. Eng.* 10, 1–8 (1972). https://doi.org/10.1016/0025-5416(72)90059–6.

[7] A. Neubrand and J. Neubrand, "Gradient materials: an overview of a novel concept", *Zeitschrift für Metallkunde* 88, 358–371 (1997).

[8] M. Koizumi, "The Concept of FGM", *Ceramic Transactions, Functionally Gradient Materials* 34, 3–10 (1993).

[9] M. Koizumi, "FGM activities in Japan", *Compos. Part B-Eng.* 28, 1–4 (1997). https://doi.org/10.1016/S1359–8368(96)00016–9.

[10] M. Wachowski, W. Kaszuwara, A. Miazga, K. Konopka, and J. Zygmuntowicz, "The possibility of producing graded $Al_2O_3$-Mo, $Al_2O_3$-Cu, $Al_2O_3$-W composites using CSC method" *Bull. Pol. Ac.: Tech.* 67, 179–184 (2019). https://doi.org/10.24425/bpas.2019.128603.

[11] M. Rozmus, „Cermetalowe materiały gradientowe", *Materiały Ceramiczne* 4, 142–147 (2006) [in Polish].

[12] B. Ilschner, "Structural and compositional gradients: basic idea, preparation, applications", *Journal de Physique IV Colloque* 3, 763–772 (1993). https://doi.org/1051/jp4:19937121.

[13] J. Zygmuntowicz, A. Miazga, P. Wiecieńska, W. Kaszuwara, K. Konopka, and M. Szafran, "Combined centrifugal-slip casting method used for preparation the Al2O3-Ni functionally graded composites", *Compos. Part B-Eng.* 141, 158–163 (2018). https://doi.org/10.1016/j.compositesb.2017.12.056

[14] J. Palka and G. Matula, *Funkcjonalne materiały gradientowe jako sposób łączenia niekomplementarnych własności mechanicznych*, PSKN, 2007

[15] K.K. Chawla, *Composite materials science and engineering*, New York: Springer Science Business Media, 2012.

[16] R. Barretta, L. Feo, and R. Luciano, "Torsion of functionally graded nonlocal viscoelastic circular nanobeams", *Compos. Part B-Eng.* 72, 217–222 (2015). https://doi.org/10.1016/j.compositesb.2014.12.018.

[17] R. Barretta, L. Feo, R. Luciano, F. Marotti de Sciarra, and R. Penna, "Functionally graded Timoshenko nanobeams: a novel nonlocal gradient formulation", *Compos. Part B-Eng*, 100, 208–219 (2016). https://doi.org/10.1016/j.compositesb.2016.05.052.

[18] X.J. Xu, and J.M. Meng, "A model for functionally graded materials", *Compos. Part B-Eng.* 145, 70–80 (2018). https://doi.org/10.1016/j.compositesb.2018.03.014.

[19] L. Dobrzański and G. Matula, „Podstawy metalurgii proszków i materiały spiekane", *Gradientowe materiały narzędziowe*, Open Access Library, 14, 56–74 (2012) [in Polish].

[20] L. Dobrzański, A. Kloc-Ptaszna, G. Matula, and J. Torralba, „Wpływ stężenia węgla na strukturę i własności gradientowych materia-łów narzędziowych", *Archiwum Odlewnictwa*, Katowice, PAN-Katowice, 2006 [in Polish].

[21] W.H. Tuan and R.J. Brook, "Processing of Alumina/Nickel Composites", *J. Eur. Ceram. Soc.* 10, 95–100 (1992). https://doi.org/10.1016/0955–2219(92)90123-U.

[22] M. Wośko, B. Paszkiewicz, T. Piasecki, A. Szyszka, R. Paszkiewicz, and M. Tłaczała, "Applications of functionally graded materials in optoelectronic devices", *Optica Applicata* 35, 663–667 (2005).

[23] T. Ogawa, Y. Watanabe, H. Sato, I.S. Kim, and Y. Fukui, "Theoretical study on fabrication of functionally graded material with density gradient by a centrifugal solid-particle method", *Compos. Part A-Appl. S.* 37, 2194–2200 (2006). https://doi.org/10.1016/j.compositesa.2005.10.002.

[24] S.S. Tjong and Z. Ma, "Microstructural and mechanical characteristics of in situ metal matrix composite", *Mater. Sci. Eng.* 29, 49–114 (2000). https://doi.org/10.1016/S0927–796X(00)00024–3.

[25] M. Szafran, K. Konopka, E. Bobryk, and K.J. Kurzydłowski, "Ceramic matrix composites with gradient concentration of metal particles", *J. Eur. Ceram. Soc.* 27, 651–654 (2007). https://doi.org/10.1016/j.jeurceramsoc.2006.04.046.

[26] A. Mortensen and S. Suresh, "Functionally graded metals and metal-ceramic composites: Part I", *Processing. Inter. Mater. Rev.* 40, 239–265 (1995). https://doi.org/10.1179/imr.1997.42.3.85.

[27] P. Grant, I. Palmer, and I. Stone, "Spray formed aerospace alloys are high flyers", *Mater. World* 7, 331–333 (1999).

[28] S. Nai, M. Gupta, and C. Lim, "Synthesis and wear characterization of Al based, free standing functionally graded materials: effect of different matrix compositions", *Compos. Sci. Technol.* 63, 1895–1909 (2003). https://doi.org/10.1016/S0266–3538(03)00158–1.

[29] J. Vleugels, G. Anné, S. Put, and O. van der Biest, "Thick plate-shaped $Al_2O_3/ZrO_2$ composites with continuous gradient processed by electrophoretic deposition", *Mater. Sci. Forum* 423, 171–176 (2003). https://doi.org/10.4028/www.scientific.net/MSF.423–425.171.

[30] J. Lackner, W. Waldhauser, R. Ebner, B. Major, and T. Schöberl, "Structural, mechanical and tribological investigations of pulsed laser deposited titanium nitride coatings", *Thin Solid Films* 453–454, 195–202 (2004). https://doi.org/10.1016/j.tsf.2003.11.106.

[31] J. Zygmuntowicz, M. Wachowski, A. Miazga, K. Konopka, and W. Kaszuwara, "Characterization of Al2O3/Ni composites manufactured via CSC technique in magnetic field", *Compos. Part B-Eng.* 156, 113–120 (2019). https://doi.org/10.1016/j.compositesb.2018.08.079

[32] O. Odawara, "Centrifugal Casting, Concise Encyclopedia of Self-Propagating High-Temperature Synthesis", *History, Theory, Technology, and Products* 58–60 (2017) https://doi.org/10.1016/B978-0-12-804173-4.00025-9

[33] J. Zygmuntowicz, A. Miazga, K. Konopka, and W. Kaszuwara, "Metal particles size influence on graded structure in composite Al2O3-Ni", *Mater. Techn.* 50, 537–541 (2016). https://doi.org/10.17222/mit.2015.120.